www.czasopisma.pan.pl PAN www.journals.pan.pl
POLSKA AKADEMIA NAUK

JOURNAL OF WATER AND LAND DEVELOPMENT
e-ISSN 2083-4535

Polish Academy of Sciences (PAN), Committee on Agronomic Sciences
Section of Land Reclamation and Environmental Engineering in Agriculture
Institute of Technology and Life Sciences (ITP)

JOURNAL OF WATER AND LAND DEVELOPMENT
2020, No. 46 (VII–IX): 216–228
https://doi.org/10.24425/jwld.2020.134216

Available (PDF): http://www.itp.edu.pl/wydawnictwo/journal; http://journals.pan.pl/jwld

Received 04.01.2020
Reviewed 23.01.2020
Accepted 17.02.2020

The impact of production of silver nanoparticles using soil fungi and its applications for reducing irrigation water salinity

Rabaa YASEEN[1)] ✉, Yousra H. KOTP[2)], Doaa EISSA[3)]

[1)] Desert Research Center, Soil Fertility and Microbiology Department, Water Resources and Desert Soils Division, P.O. Box: 1, El-Matareya 11753, Cairo, Egypt.
[2)] Desert Research Center, Department of Hydrogeochemistry, Water Resources and Desert Soils Division, Cairo, Egypt.
[3)] Desert Research Center, Department of Soil Physics and Chemistry, Water Resources and Desert Soils Division, Cairo, Egypt.

For citation: Yaseen R., Kotp Y., Eissa D. 2020. The impact of production of silver nanoparticles using soil fungi and its applications for reducing irrigation water salinity. Journal of Water and Land Development. No. 46 (VII–IX) p. 216–228. DOI: 10.24425/jwld.2020.134216.

Abstract

In the present work, the dried biomass of soil isolated fungus *Eurotium cristatum* was used for synthesizing silver nanoparticles (AgNPs). The synthesized AgNPs were spherical in shape with average diameter of 16.56 nm and displayed maximum absorbance at 418. Fourier transform infrared (FTIR) study indicated the presence and binding of proteins with myco-produced silver nanoparticles. The optimum conditions for AgNPs biosynthesis were found to be at temperature of 40°C, pH of 8.0, substrate concentration of 500 ppm and fungal biomass wt. of 0.8 g. The AgNPs showed antibacterial activity against *Staphylococcus aureus*, *Listeria monocytogenes*, *Escherichia coli* and *Shigella flexneri*. AgNPs was built-in thin film nanocomposite (TFNC) membrane and the impacts of nanomaterial composition on membrane properties and desalination process were studied. The AgNPs produced membrane TFNC had better filtration performances than pure thin film composite membrane TFC. The TFNC membrane had enhanced water flux (32.0 vs. 16.5 $dm^3 \cdot m^{-2} \cdot h^{-1}$) and advanced NaCl rejection (91.7 vs. 89%) compared to the TFC membrane. A pot experiment was conducted to evaluate the effect of the irrigation with desalinated water on yield and productivity of essential oil of the sweet basil (*Ocimum basilicum* L.) and lavender (*Lavandula multifida* L.). The irrigation with desalinated water reduced significantly the soil reaction, soil electrical conductivity (EC), sodium adsorption ratio and exchangeable sodium percent in rhizospheric soil, it also enhanced the growth and oil yield of both plants compared with those irrigated with salt water.

Key words: *antimicrobial activity, dehydrogenase, mycoynthesized nano-silver, nitrate reductase, reverse osmosis, soil salinity, water desalination*

INTRODUCTION

Egypt is among countries facing water scarcity due to its limited water resources and dryness. Agriculture consuming more than 80% of available fresh water. Thus creating new water sources for irrigation purposes becomes essential to overcome this problem. Desalination is a technical method to increase the availability of freshwater in coastal areas with limited water resources to meet the huge needs for irrigation water in this area [BELTRÁN, KOO-OSHIMA 2006]. One such area is Marsa Matrouh, located on the north western coast of Egypt. In this area the irrigation depends on both rainfall, which is minimal in most months of the year, and ground water, which often contains a high proportion of salt especially sodium.

Salts dissolved in the soil water can reduce crop growth and yield in two ways: by osmotic influences and by specific-ion toxicities. Salinity can also affect crop growth through the specific-ion toxicities of chloride, boron, and sodium ions on plants by, which occurs when these constituents in the soil water are absorbed by the roots and accumulate in the stems or leaves of plant [GRATTAN *et al*. 2015].

Soil reaction (pH) and electrical conductivity (*EC*) and the sodium adsorption ratio (*SAR*) in irrigation water are very important categories because they define the tendency of irrigation water to change the soil into sodic one. Economically, extension of salt-affected soils induces about US$ 12 billion annual global income loss [GHASSEMI *et al.* 1995]. Worldwide, there are about 95 mln ha under primary salinization inherited from the prevailing aridity. They are dominated by high atmospheric temperature and low rainfall accompanied by gradual salt efflorescence and accumulation on land surface due to the net upward water movement and evaporation. On the other hand, secondary salinization due the negative and irrational human impact as well as the ever rising of ground water effect on around 77 mln ha [GRATTAN *et al*. 2015].

Membrane technology has rapidly evolved and played a key role in the desalination and purification of water. Many researches have given more attention on reverse osmosis (RO) membranes and the physicochemical possessions of their shell. In the RO process, a higher external pressure is applied to overcome the osmotic pressure of saltwater, and reverse its flow so fresh water would pass through a semi-permeable membrane, resulting in the removal of salts. The RO process is effective for eliminating total dissolved solids (TDS) at concentrations up to 45,000 $mg \cdot dm^{-3}$ [AL-KARAGHOULI *et al.* 2009]. However, the fouling and biofouling are represent great problem faced this kind of membrane due to the deposition and adsorption phenomenon of the constituents and the formation of biofilm on membrane surface. Many researches have studied the effect of the nanoparticles incorporation into polymeric membrane matrix on the biofouling properties [REHAN *et al*. 2016; YIN *et al*. 2013]. Ag self-produced RO film prepared by phase inversion was extremely efficient in water desalination but, it was established that this kind of membrane has a problem with a release of silver from membrane face. Chemical reaction process was engaged to synthesize AgNPs in the existence of stabilizing mediator to avoid the unnecessary colloids agglomeration. In addition, AgNPs from chemical combination are painstaking hazardous to the surroundings, costly and use high energy [KOTP 2017].

Among methods used for formation of silver nanoparticle other than that of physical and chemical methods is the biological one. This method is safer and better process for nanoparticles biosynthesis as it consider as ecofriendly, low-cost and easy way giving high yield of nanoparticles. Microorganisms like fungi are effective for synthesizing silver nanoparticles intracellularly and extracellularly as they produced many enzymes [SANGAPPA, THIAGARAJAN 2012].

This study aims to a) investigate the improvement effect of incorporation myco-synthesized silver nanoparticles on reverse osmosis membrane properties and its efficacy for water desalination, b) evaluate the effect of desalinated water on the growth, yield and productivity of essential oil of sweet basil (*Ocimum basilicum* L.) and lavender (*Lavandula multifida* L.) plants and c) evaluate the role of the desalination process in the prevention of soil change into sodic one.

MATERIAL AND METHODS

MATERIALS

Polysulfone (PSf, Mw = 78,000 $g \cdot mol^{-1}$, density = 1.24 $g \cdot cm^{-3}$ at 25°C) was applied from Solvay advanced polymer, N,N-dimethylacetamide (DMAC, 99.8%, density = 0.94 $g \cdot cm^{-3}$ at 20°C) as solvent was supplied from Fisher, m-phenylenediamine (MPD, 499%), trimesoyl chloride (TMC, 498.5%), and hexane (HPLC grade, 97%) were all obtained from Sigma-Aldrich. Silver nitrate ($AgNO_3$), sodium chloride (NaCl) was obtained from Uni-Chem, and nitric acid (HNO_3, 69%) was provided by VWR Chemicals (Dorset, U.K.). Media were obtained from Oxoid (UK). Water (18.2 MΩ cm at 25°C) used to prepare all solutions was purified with a NANO pure® Diamond™ UV water system. Soil samples used for isolation were brought from the North-West and the South-West of El-Minya, Egypt. All the materials needed for microbiological experiments were purchased from HIMEDIA, including the component of potato dextrose agar (PDA) medium (used for fungal isolation), potatoes extract 200 $g \cdot dm^{-3}$, dextrose 20 $g \cdot dm^{-3}$ and agar 20 $g \cdot dm^{-3}$, and yeast extract-malt extract broth medium (used for biomass production), glucose 10 $g \cdot dm^{-3}$, sucrose 10 $g \cdot dm^{-3}$, malt extract 3 $g \cdot dm^{-3}$, yeast extract 3 $g \cdot dm^{-3}$, peptone 5 $g \cdot dm^{-3}$, pH value = 7.2. All reagents and chemicals utilized in this work were of analytical grade purity.

MICROORGANISM

Thirty two fungal isolates were used in the present work. They were isolated from serially diluted soil samples using potato dextrose agar (PDA) medium. The purified fungal isolates were screened for Ag nanoparticles production. The most potent fungal isolate was identified based on the standard taxonomic keys and monographs described by PITT and HOCKING [2009].

PRODUCTION OF FUNGAL BIOMASS

The fungal isolates were inoculated into 100 cm^3 Erlenmeyer flask containing 50 cm^3 yeast extract-malt extract broth medium. Potassium nitrate (0.5 $g \cdot dm^{-3}$) was added to the growth medium in order to stimulate the production of nitrate reductase enzyme complex. After incubation period, the fungal mat was collected by centrifugation at 6000 rpm for 10 min at 4°C. The cell biomass was washed thrice with sterile distilled water and vacuum dried at 50°C and was used for silver nanoparticle synthesis.

SYNTHESIS OF SILVER NANOPARTICLES

The most efficient fungal isolate able to synthesis AgNPs, was screened. Dried fungal biomass (0.5 g) was inoculated into 100 cm^3 Erlenmeyer flask containing 50 cm^3 of 100 mM $AgNO_3$ solution and incubated at 45°C for 48h at dark. Un-inoculated flask served as control, was incubated under the same condition as inoculated flask.

After incubation period, the solution was filtered by membrane filtration technique.

CHARACTERIZATION OF SILVER NANOPARTICLES

The particle size of freshly synthesized AgNPs was measured using dynamic light scattering (DLS). UV–VIS spectrophotometer was used to determine the absorption peak of silver nanoparticles. TEM (JEOL GEM-1010 transmission electron microscope at 70 kV at the Regional center for Mycology and Biotechnology (RCMB), Al-Azhar Univerity) was used to define the shape and size distribution of AgNPs. The functional groups of dried fungal mat, silver nitrate and that present on the surface of the membranes were evaluated by Fourier transform infrared (FT-IR) spectroscopy (Nicolet avatar 230 spectrometers) at room temperature. Powder X-ray diffraction (XRD) patterns were made by (Shimadzu X-ray diffractometer, Model XD 490 Shimadzu, Japan).

FACTORS AFFECTING AgNPs PRODUCTION

The optimum operating conditions for the synthesis of AgNPs were determined to attain the maximum production of silver nanoparticles. The investigated conditions are biomass weight (cell free filtrate, 0.2, 0.5 and 0.8 g dry mass), temperature (20, 30, 40 and 50°C), pH (5, 6, 7, 8, 9 and 10) and the concentration of silver nitrate (1.18, 1.77, 2.94, 4.12 and 5.89 mM). The absorbance of resulting samples was estimated at 418 nm.

ANTIBACTERIAL PROPERTIES OF PRODUCED AgNPs

The antimicrobial activities of AgNPs against the Gram positive bacteria (*Staphylococcus aureus* and *Listeria monocytogenes*) and the Gram negative bacteria (*Escherichia coli* and *Shigella flexneri*), were determined by agar plate well diffusion assay on nutrient agar (NA) medium.

DETERMINATION OF HYDROLYTIC ENZYME ACTIVITIES

For determination of intracellular enzyme activities, fungal mat was washed with sterilized distilled water for at least 10 times. The mat was dried and grounded with acid-washed quartz sand in a mortar. Dehydrogenase activity was assayed by a modification of the method of [KLEIN *et al.* 1971], in brief 0.2 cm^3 of 3% triphenyltetrazolium chloride and 0.5 cm^3 of 1% glucose solution were added to one gram of fungal mat and were incubated at 28°C for 24 h. After incubation, 5 cm^3methanol was added and again incubated in dark at 28°C for one h. The absorbance of triphenyl formazan (TPF) was measured at 485 nm on a spectrophotometer.

Nitrate reductase activity in the fungal mat was assayed according to the procedure described by [HARLEY 1993] with modification. Succinctly, fungal mat (0.1 g) was added to an assay medium (30 mM KNO_3 and 5 $cm^3$of 0.1 M phosphate buffer pH 7.5) and incubated in dark at 30°C, for 1 h. After incubation, nitrite was determined in the filtrate by adding 1 cm^3 of 1% sulphanilamide and 1 cm^3 of 0.05% N-(1-naphthyl) ethylene diaminedihydrochloride. The absorbance of the developed pink azo-dye was measured after 30 min by UV–visible spectrophotometry, at 540 nm. Standard nitrite solutions were prepared in the same way.

PREPARATION OF THIN FILM COMPOSITE (TFC) AND THIN FILM NANOCOMPOSITE (TFNC) MEMBRANES

Polysulfone (PSf) casting solutions (16 wt. % were dissolved in N,N-dimethylacetamide DMA). The amounts of AgNPs were added to the polysulfone casting solution and the concentration varied from 0.0 to 0.3 wt. % was sonicated for 2 h. A film of PSf was cast by spreading the PSf solution on top of a glass and doped in deionized water at 298 K. TFC membrane fabricated by using pure PSf (containing zero concentration of silver nanoparticles, and TFNC membrane containing different concentrations of AgNPs were immersed in an aqueous solution of 2.0 wt. % m-phenylenediamine (MPD) for 2 min. Next, the MPD saturated PSf and Ag/polysulfone support layer was soaked in an organic solution of 0.15wt. % of TMC-hexane for 60 s, completing the construction of a polyamide (PA) film. The equipped membranes were cleaned with DI water before testing.

WATER SAMPLING AND ANALYSIS

The saline water sample was brought from well in Marsa Matrouh, located on the north western coast of Egypt, at 31°42’96.00” N, and 26°17’77.00” E. Different parameters such as pH, *EC*, soluble cations (Na^+, K^+, Ca^{2+}, Mg^{2+}), soluble anions (CO_3^{2-}, HCO_3^-, Cl^-, SO_4^{2-}) and heavy metals contents in water samples (untreated irrigation water, treated irrigation water and tap water) were determined.

SOIL SAMPLING AND ANALYSIS

The soil sample under consideration represents the epipedon (0–50 cm) was obtained from Ismailia Governorate, Egypt. The soil was air dried, crushed, and sieved through a 2-mm sieve. Soil texture was determined using international pipette method [USDA 2014]. Soil organic matter content, pH and *EC* were verified in the soil paste and its minerals content were determined using flame spectrophotometer and inductivity coupled argon plasma (ICAP) after digestion of the samples with a ternary acids mixture of HNO_3, H_2SO_4 and $HClO_4$ according to USDA [2014]. The sodium adsorption ratio (*SAR*) was calculated for the 50-cm soil matrix according to USDA [2014]:

SAR was estimated using the equation (1),

$$SAR = \frac{Na}{\sqrt{\frac{Ca+Mg}{2}}} \quad (1)$$

Where the ionic concentration of the saturation extracts is expressed in meq·dm^{-3}.

The exchangeable sodium percentage (*ESP*) was estimated using the equation (2):

$$ESP = \frac{100(-0.0126+0.01475SAR)}{1+(-0.0126+0.01475SAR)} \quad (2)$$

POT EXPERIMENT

A pot experiment was conducted during the cropping season 2018–2019 to investigate the effect of the irrigation with desalinated water on yield and productivity of essential oil of the sweet basil (*Ocimum basilicum* L.) and lavender (*Lavandula multifida* L). Three treatments comprising T1: salt water (SW); T2: desalinated water (DSW) and T3: tap water (control) were applied with ten replicates. The chemical analysis of water types used for irrigation was determined according to USDA [2014]. The sweet basil and lavender seedlings (25 days old) were planted in the pots containing 8 kg soil. The fertilizers were applied as the same for all treatments (as ammonium sulphate, calcium superphosphate and potassium sulphate). Plants were irrigated three times per week with 100 cm^3 of each water treatment, which was sufficient to drain from the bottom of all pots. After 125 days from planting, the sweet basil and lavender plants were cut at the soil surface and washed with deionized water. Plants were oven-dried at 70°C for 48 h, weighed for dry matter yield, and grounded. Plants and soil samples of different treatments were digested using H_2SO_4–H_2O_2 according to USDA [2014]. The minerals content in digestive samples were analysed by flame spectrophotometer and ICAP.

STATISTICAL ANALYSIS

Data of the present work were statistically analysed and the differences between the means of the treatments were considered significant when they were more than the least significant differences (LSD) at the 5% level by using computer program of Statistic version 9. The treatments were used in a completely randomized design.

RESULTS AND DISCUSSION

SOIL FUNGI ISOLATION, IDENTIFICATION AND SCREENING FOR BIOSYNTHESIS OF AgNPs

Thirty two fungal isolates were screened for Ag nanoparticles production. The fungal isolate able to synthesis AgNPs numbered as UA13 was selected based on the particle stability and faster rate of synthesis. The fungal isolate that could synthesize AgNPs, was identified according to its morphological and microscopical features. It showed low growth rates (3–4 cm per 10 days) with golden yellow to yellowish grey color while reverse is pale or dark green on Czapek Dox agar medium. The texture of fungal colonies is cottony to somewhat granular. Conidiophore was smooth, some shade of brown and conidia were spherical and was borne in radiate to loosely columnar heads. Based on these typical characteristics, the isolate was found to belong to species *Eurotium cristatum* (Photo 1).

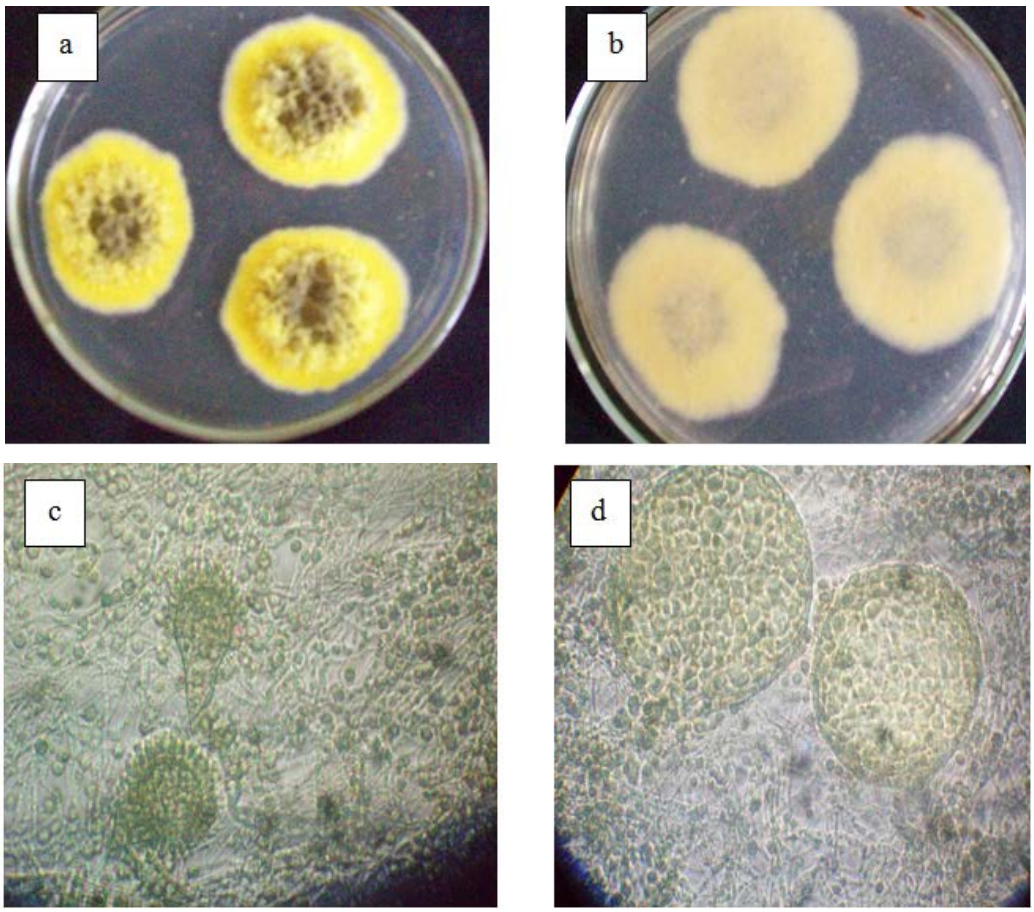

Photo 1. *Eurotium cristatum*: a), b) colonies on Czabek's agar medium, c) asexual fruiting structure illustrating conidiophore, vesicle, phialides and conidiospores, d) mature cleistothecium releasing ascospore (sexual reproduction) (phot. *R. Yaseen*)

CHARACTERIZATION OF SILVER NANOPARTICLES

TEM examination of the silver nanoparticles utilized in this effort (Fig. 1a), showed that, the particles were well detached and had spherical morphology with average diameter of 16.56 nm. The existence of silver nanoparticles was confirmed by UV–Vis spectrometer as exposed in Figure 1 b, a particular broad peak was observed, centered at 418 and 436 nm which owed to the plasmon excitation of the silver nanoparticles [YIN *et al*. 2013]. Figure 1c showed the Fourier transform infrared (FTIR) spectrum recorded from the freeze-dried powder of silver nanoparticles, bioformed after 72 h of incubation with the fungus. The amide linkages connecting amino acid residues in proteins provide the well-known signatures in the infrared region of the electromagnetic spectrum. The bands observed at 3420 cm^{-1} and 2921 cm^{-1} were assigned to the stretching vibrations of primary and secondary amines, correspondingly; while their corresponding bending vibrations were observed at 1698 cm^{-1} and 1558 cm^{-1}, respectively [SOLIMAN *et al*. 2019]. The two bands seen at 1380 cm^{-1} and 1026 cm^{-1} may be assigned to the C–N stretching vibrations of aromatic and aliphatic amines, respectively. The overall examination proves the occurrence of protein in the samples of silver nanoparticles. X-ray diffraction (XR) guide of the dried silver nanoparticles (Fig. 1d). In XRD spectrum the diffractions at 2θ 32°, 41.2° and 67.2° 2θ can be indexed to the (111), (200) and (220) planes of the face-centered cubic silver, respectively. At the same time as two new peaks (*) are created due to the interaction of silver with the fungal cell wall.

OPTIMIZATION OF REACTION CONDITIONS OF AgNPs BIOSYNTHESIS

The biosynthesis of the AgNPs was optimized by standardizing the effects of pH, temperature, $AgNO_3$ concentration and fungal biomass concentration. The optimum pH value for AgNPs biosynthesis was determined, a pH ranged from 5–9 was tested in this study. Results in Figure 2a showed that there is an increase in absorbance as pH increased, suggesting that an alkaline habitat was more appropriate for AgNPs biosynthesis. The hydrogen ion concentration in the reaction mixture greatly affected the AgNPs biosynthesis, this may be because the microbial enzymatic activities were greatly influenced by hydrogen

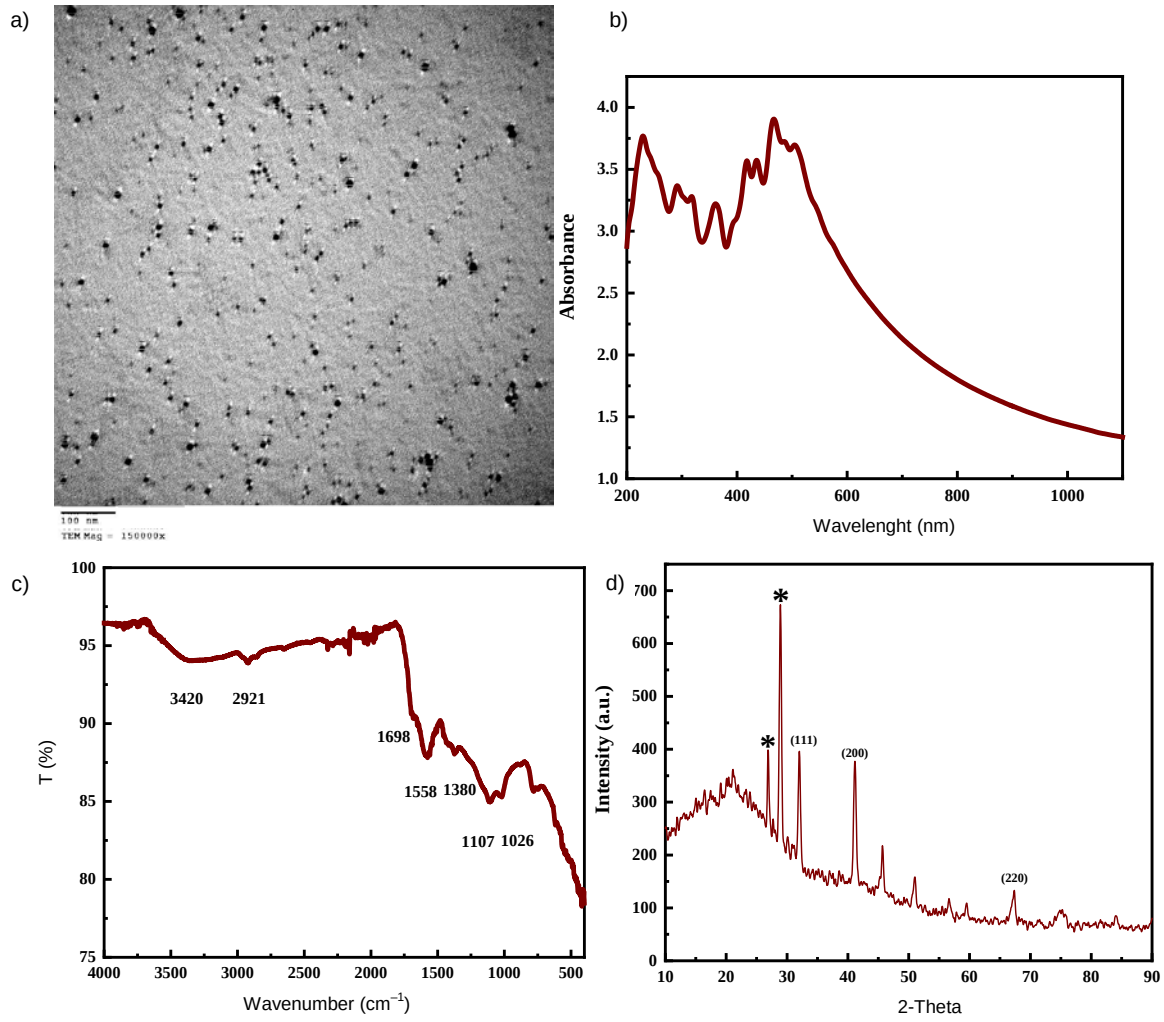

Fig. 1. Characterization of myco-synthesized AgNPs: a) TEM image of AgNPs, b)UV–vis absorption spectrum, c) FTIR spectra, d) XRD pattern of AgNPs; source: own study

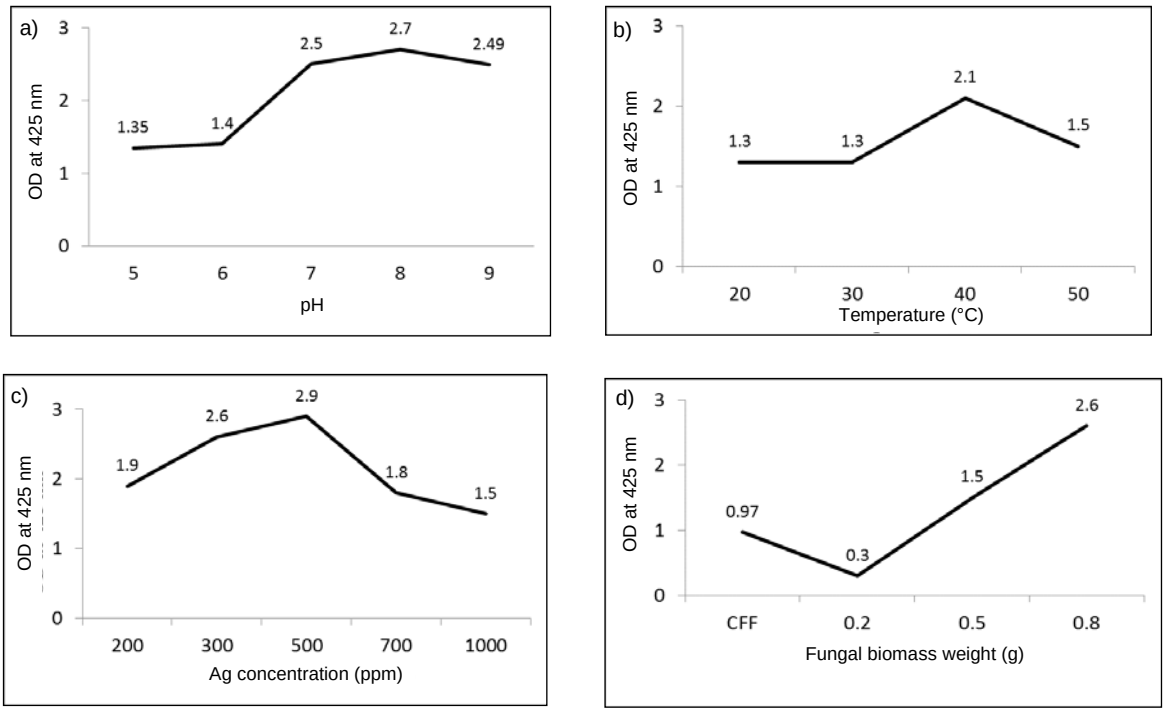

Fig. 2. Optimization of green synthesis of silver nanoparticles from *Eurotium cristatum*; CFF = cell free filtrate; source: own study

ion [YASEEN, YOSSIF 2019]. Regarding the optimal temperature for AgNPs biosynthesis, the absorbance measurements indicated that the optimum temperature was 40°C, the AgNPs production was reduced at higher temperatures as demonstrated by Figure 2b. Different substrate concentrations of $AgNO_3$ in the reaction mixture had an obvious influence on the biosynthesis of AgNPs, and 500 ppm was the optimum concentration. The AgNPs biosynthesis decreased with an increase in substrate concentration above 500 ppm (Fig. 2c). Absorbance values also increased with increasing the weight of fungal inoculum, up to 0.8 g (Fig. 2d). Similar results were obtained by [SANGAPPA, THIAGARAJAN 2012] who found that the optimum conditions for AgNPs biosynthesis were a temperature 37°C, a pH of 6.0 and a substrate concentration of 2.0 mM while [FOUDAA *et al*. 2017] obtained the maximum yield of AgNPs when fungal Biomass filtrate treated with 1.5 mM of $AgNO_3$ silver nitrate at pH 10 and incubated at 35°C for 24 h.

ANTIBACTERIAL PROPERTIES OF PRODUCED AgNPs

The biofouling is one of the most problems that faced reversed osmosis membrane due to the formation of bacterial biofilm on membrane surface [REHAN *et al*. 2016]. The antibacterial effect of myco-synthesized AgNPs was evaluated and data revealed that AgNPs showed strong inhibitory effect against common food-borne pathogens, including *S. aureus*, *L. monocytogenes*, *E. coli* and *S. flexneri* revealing 12, 17, 16.3 and 15 mm inhibition zones, respectively (Tab. 1). Both Gram-positive and -negative bacteria have different vulnerability to AgNPs, probably due to variations in their membranes and cell walls structure [OTTONI *et al*. 2017].

Table 1. The inhibitory effect of silver nanoparticles against various bacterial pathogens

Pathogen		Inhibition zone (mm)
Gram positive	*Staphylococcus aureus*	12±1
	Listeria monocytogenes	17±2.2
Gram negative	*Escherichia coli*	16.3±0.6
	Shigella flexneri	15±1

Source: own study.

DETERMINATION OF HYDROLYTIC ENZYME ACTIVITIES

The reduction of Ag^+ to Ag^0 was mediated by the biomolecules produced by *E. cristatum*. The activities of dehydrogenase and nitrate reductase were determined in dried fungal mat and data revealed that dehydrogenase activity was 28.4 µmol TF per g protein per h while nitrate reductase activity reached 91.51 µmol NO_2 per h per g protein (Fig. 3). Oxidation reduction reaction is the most essential enzymatic detoxification mechanism for microbial transformation of metals to their nanoscale. The reduction processes of metals often initiate by the respiratory enzymes (oxidoreductase) such as NADH-dependent nitrate reductase or NAD-linked dehydrogenases which were membrane-bounded proteins [HAMEDI *et al*. 2012]. GUILGER-CASAGRANDE *et al*. [2019] also examined the specific activity of fungal hydrolytic enzymes (β-1,3-glucanase, N-acetyl-beta-D-glucosaminidase (NAGase), chitinase and acid proteases) in samples of biogenic silver nanoparticles, they observed that the highest specific activity was obtained for NAGase, followed by β-1,3-glucanase while the specific activity of chitinase and acid protease were observed with lower values.

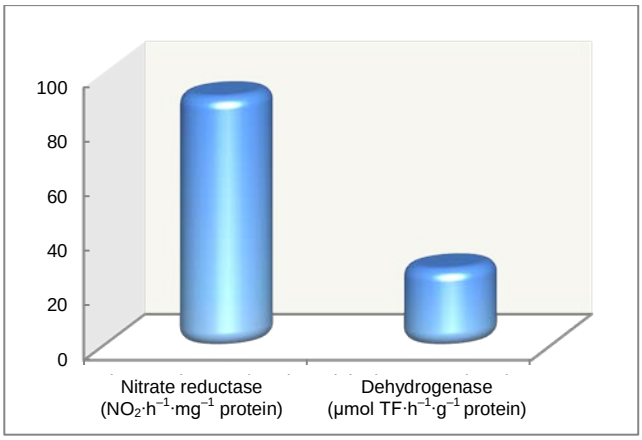

Fig. 3. Enzyme activities of *Eurotiumcristatum*; source: own study

MEMBRANE CHARACTERISTICS

Surface and cross-section of TFC and TFNC membranes were investigated by scanning electron microscope (SEM) images (Fig. 4) and showed that Ag/PSf/PA membrane had the identical ridge-and-valley arrangement of a PSf/PA membrane. At a relatively high magnification of 20000, deposits of light nanoparticles can be shown on the membrane surfaces. The SEM analysis coupled with energy dispersive X-ray spectroscopy (EDX) definitude the structure of discrete silver nanoparticles as a substitute of a continuous layer of Ag^0 deposits on the PSf support membrane (Fig. 2b). The nanoparticles, on the other hand, were unevenly widen at the microscale and different in diameter [KOTP 2017]. Most AgNPs had size less than 20 nm, but they are able to form aggregates with diameters up to 180 nm in the interior membrane. Transmission electron

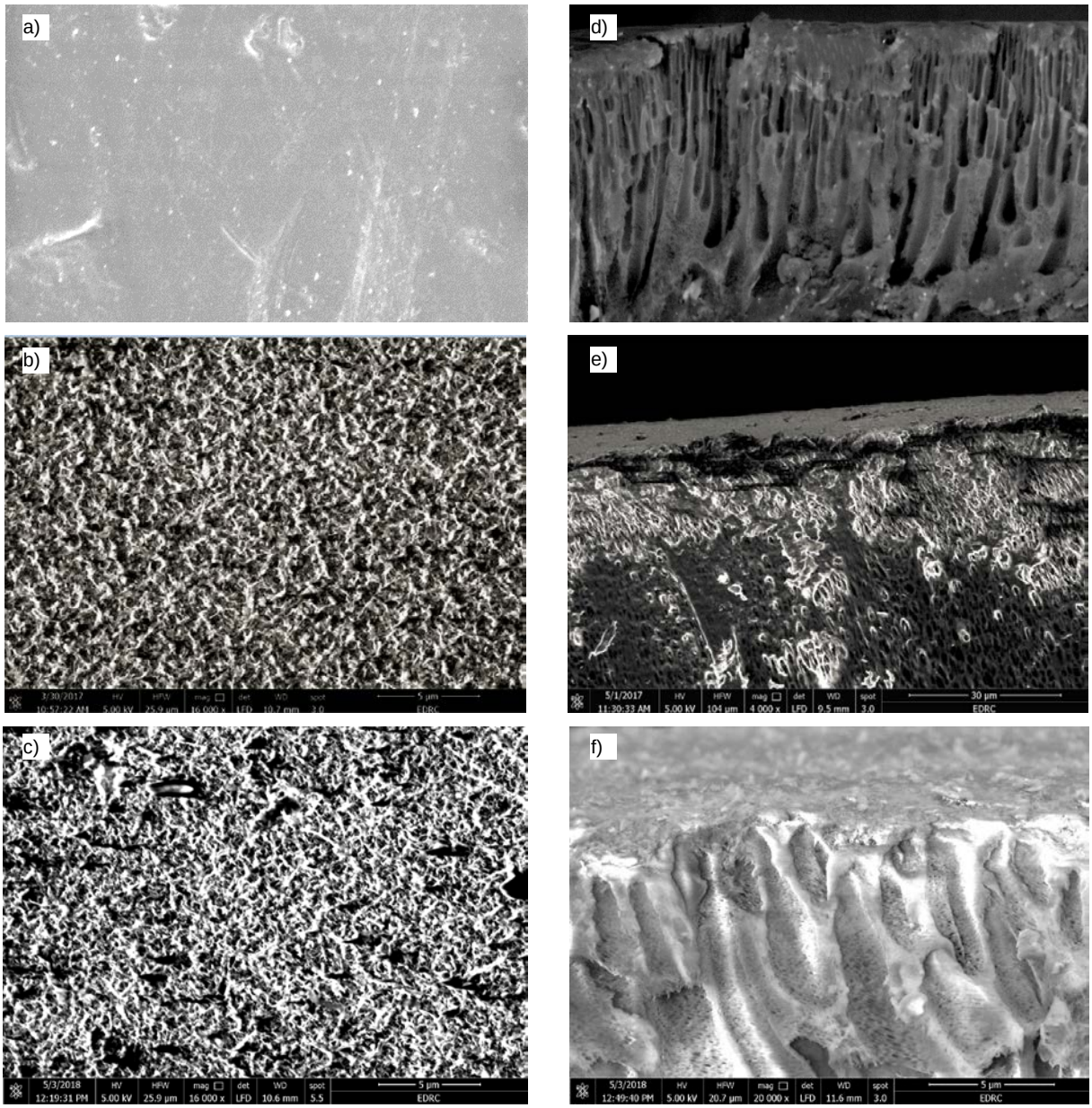

Fig. 4. SEM images of: top surface (a, b, c) and cross section (d, e, f) of polysulfone (PSf), thin film composite (TFC) and thin film nanocomposite (TFNC) reversed osmosis membrane, respectively; source: own study

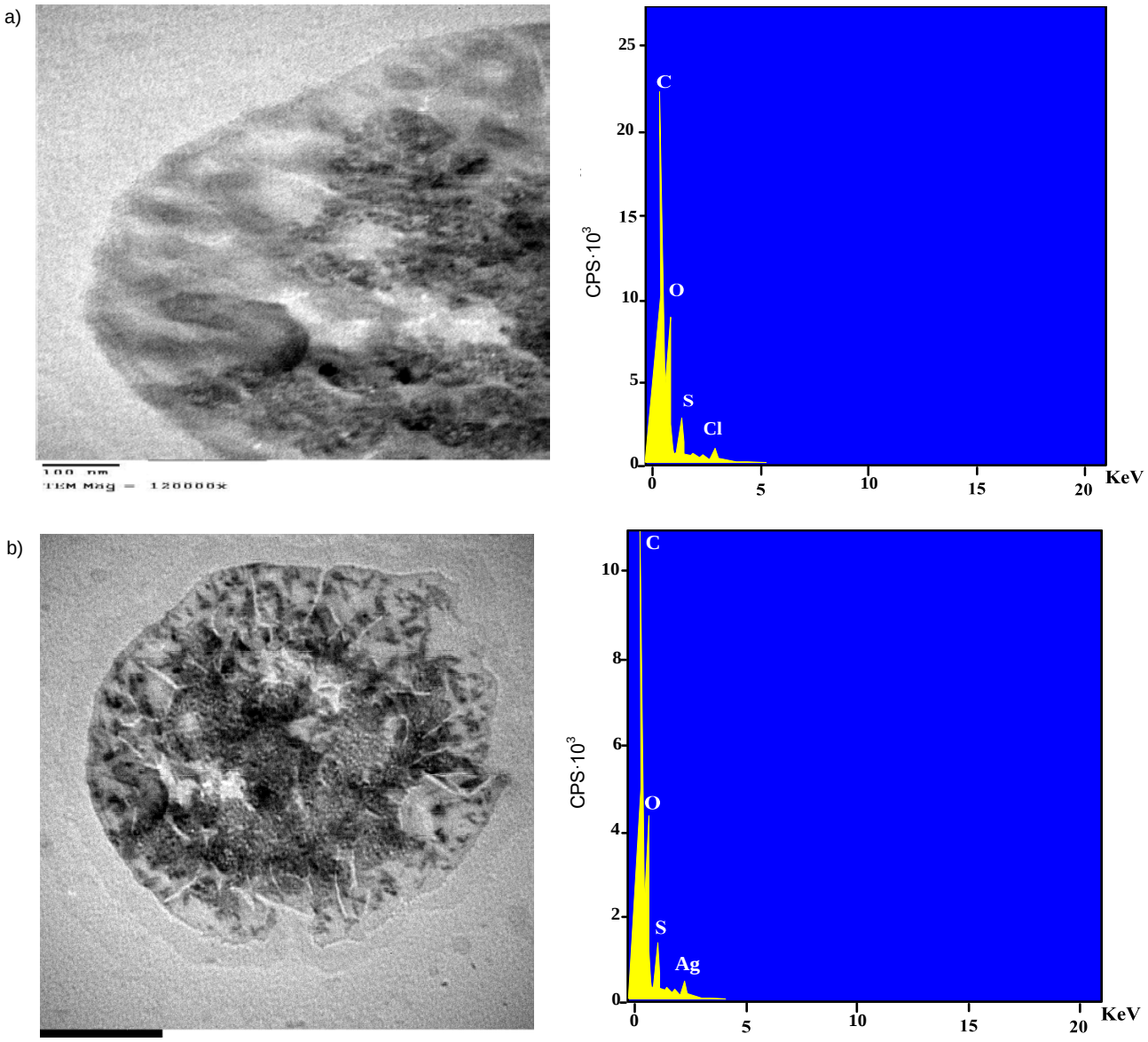

Fig. 5. Transmission electron microscope (TEM) and energy dispersive X-ray spectroscopy (EDX) images of reversed osmosis membranes: a) thin film composite (TFC), b) thin film nanocomposite (TFNC)

microscope (TEM) images and EDX spectra are available for TFC and TFNC membranes in Figure 5 (a, b). Both TFC and TFNC membranes showed nano-scale surface roughness, which is a well-known characteristic of interfacially polymerized polyamide RO membranes [MUSARRAT *et al.* 2010; AHLUWALIA *et al.* 2014]. The irregular morphology permits quantification of a single film layer thickness, except equally thin films are concerning 40–200 nm. In Figure 5b, silver nanoparticles show considerably darker than the polymer and are positioned within the cross-section of the thin film (Fig. 5d), and at the border. The EDX scale in Figure 5b points the form of the characteristic silver peak in the EDX arrangement also recognized the continuation of Ag nanoparticle in the PSf support in addition the occurrence of sulfur peak from the PSf support.

Surface crystallization of TFC and TFNC membranes were assessed by XRD, as revealed in Figure 6. XRD models of TFC (containing zero Ag nanoparticles in the PSf support layer) and TFC (containing Ag nanoparticles in the PSf support layer) membranes. Figure 5 changed with deference to Ag nanoparticles related peaks. The XRD pattern of the TFNC membrane displayed three diffraction peaks for silver: Ag (1 1 1) and Ag (2 0 0) [VRIJENHOEK *et al.* 2001]; these peaks were missing in the XRD patterns of the TFC membrane.

FT-IR spectra of PSf support layer, TFC and TFNC membranes are exposed in Figure 7. For the PSf support layer, peaks at 1586 and 1486 cm^{-1} might be assigned to aromatic C–C stretching, 1324 and 1219 cm^{-1} to the doublet from the asymmetric O=S=O stretching of sulfone group, 1231 cm^{-1} to the asymmetric C–O–C stretching of aryl ether group and1172 cm^{-1} to the symmetric O=S=O stretching of sulfone group, every one obtainable in the PSf fractious-linking polymerization [KOTP *et al.* 2017]. For TFC thin layer was covered on the PSf support layer subsequent to the induced polymerization (IP) method, and numerous new peaks showed on the spectrum (Fig. 6). Peaks at 1638 cm^{-1} (amide I, C=O stretching vibrations of

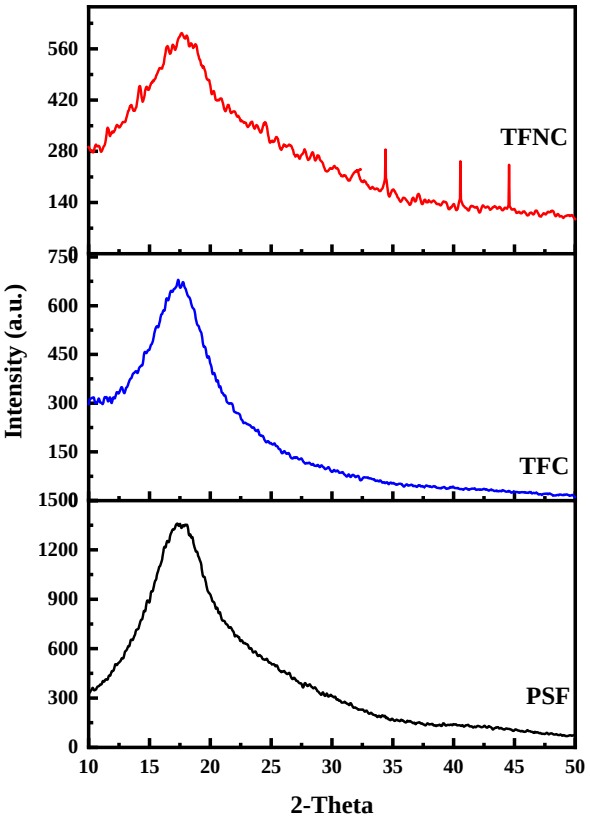

Fig. 6. X-ray diffraction (XRD) images of polysulfone (PSf), thin film composite (TFC), thin film nanocomposite (TFNC) reversed osmosis membranes; source: own study

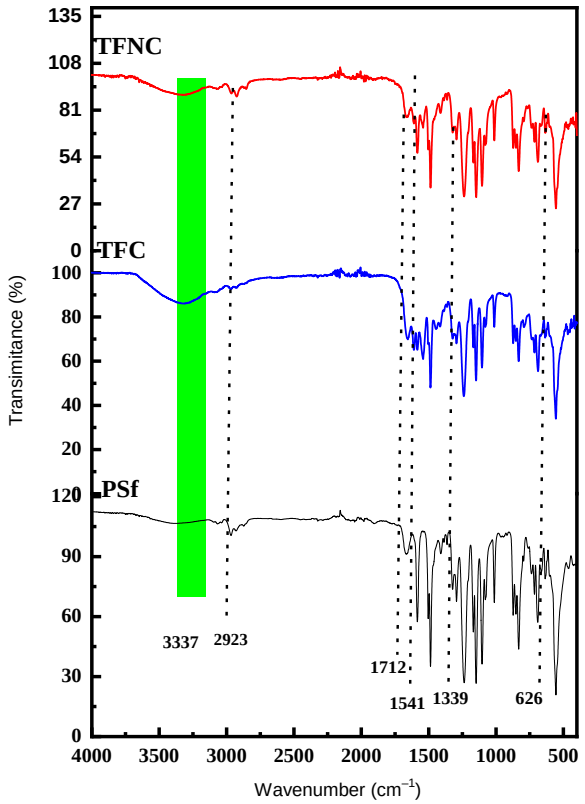

Fig. 7. Fourier transform infrared (FTIR) spectra of polysulfone (PSf), thin film composite (TFC), thin film nanocomposite (TFNC) membranes; source: own study

amide), 1577 cm^{-1} (amide II, in-plane N–H bending and C–N stretching vibrations), 1614 cm^{-1} (N–H stretching of amide II) and 1444 cm^{-1} for (C=O stretching and hydroxyl bending of carboxylic acid) were formed from the polymerization of polyamide (PA) and incorporated amide implementations [EL-AASSAR *et al.* 2017]. In addition these peaks from PA thin-film layer, the peak among 2852 and 2923 cm^{-1} resulting from the asymmetric and symmetric vibration of CH_2 groups in *E. cristatum* fungus while their bending vibrations of primary and secondary amines were illustrious at 1712 cm^{-1} and 1541 cm^{-1}, correspondingly, these both bands are narrow and strong in Ag-NPs spectrum comparative to the spectrum of fungous extract. The stretching band at 3337 cm^{-1} assures the attendance of either OH groups of algal polysaccharides or –NH groups of amide. Though, this band is extra intense and is transferred to a higher wavenumber (3420 cm^{-1}) in the spectrum of Ag-NPs [EL-AASSAR *et al.* 2017].

The metal-polymer announcement bands are marked specifically in the little frequency state (600–400 cm^{-1}). Silver exhibits a distinct new band at 626 cm^{-1} (due to metal-oxygen interaction) and a small bear band at 871 cm^{-1}. Thus, from the FTIR spectra, one can examine that metals have showing relations with the electron contributed sites, i.e., oxygen sites nearby in the polymer spine [SRIDHAR *et al.* 2007].

PERFORMANCE OF TFC AND TFNC MEMBRANE

Permeate flux from 2000 $mg \cdot dm^{-3}$ NaCl solution and salt rejections of the TFC and TFNC membranes were calculated at 1 MPa (Fig. 8). Ag/PSf/PA membrane redundant NaCl at 91.7%, which was really higher than the salt rejections of the TFC (89%). It showed that, the nano-porous establishment of PSf support layer did not allow major salt rejection. Next the IP procedure, these nano-pores were sheltered by a PA thin-film layer, which acted as a thick barrier or ejects salt ions. For the TFNC membranes, the permeate flux enlarged from 16.5 to 32 $dm^3 \cdot (m^2 \cdot h)^{-1}$ (a 100% increase) with rising AgNPs concentration start-

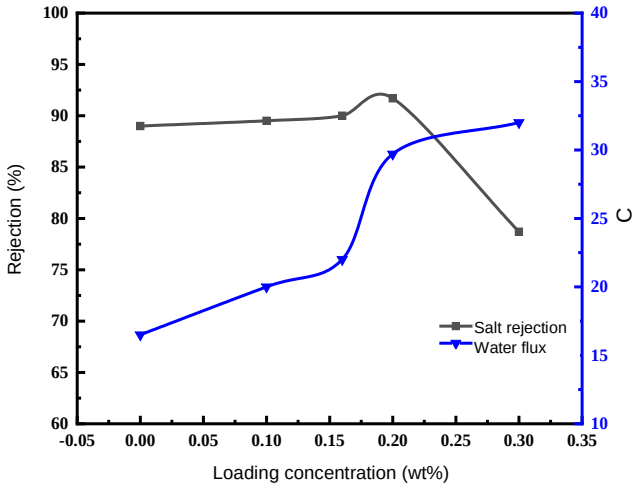

Fig. 8. Effect of AgNPs concentration on salt rejection and water flux of the resulting thin film nanocomposite (TFNC) membrane; source: own study

Table 2. Some chemical properties of water types used for irrigation

Water type	pH	*EC* (dS·m^{-1})	Cation (me·dm^{-3})				Anion (me·dm^{-3})				*SAR*	Sr ppm	B ppm
			Na^+	K^+	Ca^{2+}	Mg^{2+}	Cl^-	CO_3^{2-}	HCO_3^-	SO_4^{2-}			
T1	8.7	12.64	1 050	200	100	150	2 149	12	120	364	79.37	10.96	1.35
T2	7.8	1.03	110	8	16.8	13	170	0	85.4	30	22.79	0.211	0.012
T3	7.4	0.86	41	4	15.6	80	48.93	0	34.64	21.03	2.93	0.311	0.011

Explanations: T1 = salt water, T2 = desalinated water, T3 = tap water, *EC* = electrical conductivity, *SAR* = sodium adsorption ratio.
Source: own study.

ing from 0 to 0.3 wt%. It be capable of caused by the enlargement of membrane hydrophilicity. Moreover, the AgNPs well-established in PSf support layer is capable to change the cross-linking state of the polymer medium through producing microporous deficiency. Clearly, the membrane prepared by using 0.2wt% of AgNPs was well thought-out optimal, since the water flux increased with additional concentration increases. The declining in salt rejection with growing silver nanoparticle loading might be occurred by the accretion of AgNPs, which may take place more merely at a better concentration [SRIDHAR *et al.* 2007].

POT EXPERIMENT

A pot experiment was conducted to investigate the effect of the irrigation with desalinated water on yield and productivity of essential oil of the sweet basil and lavender. The chemical analysis of three water treatments were presented in Table 2. The main physical and chemical properties of the precultivated soil sample were summarized in Table 3. The soil texture was clay. Soil pH was 7.27, indicating neutral soil reaction. The investigated soil was non-saline, as indicated by *EC* value which was 1.61 dS·m^{-1}. Organic matter content was 0.59% and *SAR* was 2.78.

Table 3. Initial status of some chemical and physical properties of the precultivated soil

Parameter	Value
Particle size distribution (%)	
Sand (%)	25.6
Silt (%)	29.5
Clay (%)	44.9
Texture class	clay
OM (%)	0.59
pH (soil paste extract)	7.27
EC (dS·m^{-1})	1.61
Soluble ions (me·dm^{-3})	
Na^+	6.00
K^+	0.81
Ca^{2+}	5.80
Mg^{2+}	3.50
Cl^-	3.33
HCO_3^-	1.90
CO_3^{2-}	–
SO_4^{2-}	10.87
SAR	2.78
ESP	1.96

Explanations: OM = organic mass, *EC* = electrical conductivity, *SAR* = sodium adsorption ratio, *ESP* = exchangeable sodium percentage.
Source: own study.

EFFECT OF IRRIGATION WATER SALINITY ON GROWTH AND OIL CONTENT OF TESTED PLANTS

Fresh and dry weights of tested plants were significantly affected by different irrigation water as shown in Table 4. Both fresh and dry weights were decreased with increasing *EC* value of irrigation water. The fresh and dry weights were decreased by 44.1 and 26.5 respectively of sweet basil plants irrigated with salt water compared with control. The same result was obtained with lavender plant irrigated with salt water and the reduction percent in fresh and dry weight was 35.6 and 34.2 respectively. However, there was no significant difference between the control (tap water) and desalinated irrigation water treatments. Oil yield of the tested plants also affected by irrigation treatments in the same trend as the above results, the lowest mean oil percentage was obtained with salt irrigation water treatment (0.21 and 1.52%) for sweet basil and lavender, respectively. At the same time the irrigation with desalinated water increased about 229% and 103% in oil % for sweet basil and lavender respectively. These results confirm those obtained by NICOLÁS [2019], who also observed that plant growth and oil percentage were significantly affected by salinity during their work on basil and olive respectively.

EFFECT OF IRRIGATION WATER SALINITY ON K^+, Na^+ AND Ca^{2+} CONCENTRATION IN SWEET BASIL AND LAVENDER

Potassium plays a significant role in maintaining water content of tissues, beside both K^+ and Ca^{2+} are required to maintain the integrity and functioning of cell membranes [WEI *et al.* 2003], it was important to study the effect of water quality on the accumulation of K^+, Na^+ and Ca^{2+} in tested plants.

Data presented in Table 4 showed that sodium content was very high in plants irrigated with salt water (4.076 and 2.550%) for sweet basil and lavender, respectively. While Na^+ content recorded low value in plants irrigated with desalinated and tap water. Also, data showed that irrigation water with different salinity values significantly affected the K^+ content in tested plants. The lowest potassium content was obtained with tap water treatment (4.324 and 4.680%) for sweet basil and lavender, respectively. The Ca^{2+} content was increased with increasing irrigation water salinity value. The highest content in this respect was noticed with untreated water treatment (4.250 and 2.014%) followed by treated water treatment, while, the lowest content was obtained with tap water treatment (3.468 and

Table 4. Effect of irrigation water salinity on sweet basil and lavender growth characterizations (mean, n = 10)

Plant name	Irrigation water type	Plant fresh weight	Plant dry weight	Oil	Na^+ in plant	K^+ in plant	Ca^{2+} in plant	Na:Ca
		g per pot		%	%			
Sweet basil	T1	11.68 B	4.69 A	0.21C	4.076 A	6.059 A	4.250 A	0.96 A
	T2	20.21 A	5.20 A	0.71 A	0.857 B	4.682 B	4.105 B	0.20 B
	T3	20.89 A	6.38 A	0.47 B	0.807 B	4.324 C	3.468 C	0.23 B
$LSD_{0.05}$		4.810	2.35	0.101	0.954	0.990	1.36	0.027
Lavender	T1	8.25 B	4.62 B	1.52 C	2.550 A	4.894 A	2.014 A	1.27 A
	T2	14.59 A	7.19 A	3.08 A	0.826 B	4.680 B	1.816 A	0.47 B
	T3	12.81 A	7.02 A	2.30 B	0.767 B	4.680 B	1.588 B	0.48 B
$LSD_{0.05}$		2.036	0.803	0.330	0.837	1.690	2.022	0.087

Explanations: n = number of samples, LSD = least significant differences, the letters in the same column denote significant differences among the treatments, $p < 0.05$, T1–T3 as in Table 2.
Source: own study.

1.588%) for sweet basil and lavender respectively. These data are in agreement with those obtained by ASHRAF *et al.* [2016] where, Na, K and Ca ions of sunflower were increased with increased salt concentrations of irrigation water.

EFFECT OF IRRIGATION WATER SALINITY ON SOME HEAVY METALS CONTENT OF SWEET BASIL AND LAVENDER

Heavy metals are conventionally defined as elements with metallic properties and an atomic number >20. The most common heavy metal contaminants are Cd, Cr, Cu, Hg, Pb, and Zn. Metals are natural components in soil. Some of these metals are micronutrients necessary for plant growth, such as Zn, Cu, Mn, Ni, and Co, while others have unknown biological function, such as Cd, Pb, and Hg [GAUR, ADHOLEYA 2004]. The effects of water salinity on the transfer of heavy metals to tested plants were investigated. Heavy metal content was determined in all plants under investigation and data showed that salinity of irrigation water significantly affected heavy metal uptake bytested plants (Tab. 5). There were a significant decrease in heavy metal uptake by sweet basil plants irrigated with desalinated water and tap water except for Cr and Co when compared with plants irrigated with salt water. The same results were obtained from lavender plants, however, there was no significant difference in B and Cd content in all treated lavender plants. Majority of heavy metal were within the permissible limits except the Zn and Cr. The Zn and Cr contents in both plants were measured above the permissible limit recommended by WHO [2006]. Similar results were obtained by LEÓN-ROMERO *et al.* [2017] who found that NaCl solution increased both the concentration of heavy metals in soil saturation extract and their uptake by *Arabidopsis thaliana*.

Table 5. Effect of irrigation water salinity on some heavy metals content of sweet basil and lavender (mean, n = 10)

Plant name	Irrigation water type	B	Ba	Cu	Cd	Co	Cr	Fe	Mn	Ni	Pb	Sr	Zn
		ppm											
Sweet basil	T1	0.085 A	0.094 A	5.50 A	0.034 A	0.322 A	5.44 A	113.52 A	21.16 A	1.89 A	2.19 A	27.74 A	16.30 A
	T2	0.075 B	0.076 B	4.36 B	0.016 B	0.334 A	4.82 A	104.03 B	18.07 B	0.78 B	1.74 B	25.36 B	9.0 B
	T3	0.061 B	0.048 B	3.96 B	0.013 B	0.320 A	3.67 B	100.67 B	15.64 B	0.47 C	1.46 B	22.78 C	4.80 C
$LSD_{0.05}$		0.00704	0.013	0.926	0.018	0.090	0.859	8.11	1.81	0.108	0.38	1.03	4.67
Lavender	T1	0.078 A	0.023 A	4.40 A	0.022 A	0.377 A	3.67 A	114.6 A	20.22 A	0.412 A	3.242 A	14.95 A	15.70 A
	T2	0.122 A	0.014 B	2.73 B	0.012 A	0.223 B	3.08 B	106.1 B	14.84 B	0.207 B	2.167 B	11.96 B	13.0 B
	T3	0.046 A	0.009 B	2.52 B	0.019 A	0.119 C	2.50 C	97.96 C	12.92 C	0.225 B	1.898 B	10.0 C	10.50 C
$LSD_{0.05}$		0.098	0.00798	0.453	0.017	0.027	0.514	7.53	1.75	0.109	0.309	1.14	2.65

Explanations as in Table 4.
Source: own study.

Table 6. Effect of irrigation water salinity on extract of soil paste

Plant name	Irrigation watertype	pH	EC ($dS \cdot m^{-1}$)	Cation ($me \cdot dm^{-3}$)				Anion ($me \cdot dm^{-3}$)				SAR	ESP
				Na^+	K^+	Ca^{2+}	Mg^{2+}	Cl^-	CO_3^{2-}	HCO_3^-	SO_4^{2-}		
Sweet basil	T1	8.59 A	9.30 A	77.69 A	0.928 A	7.91 A	16.038 A	42.04 A	–	2.36 A	58.17 A	22.45 A	24.16 A
	T2	7.87 B	5.93 B	27.39 B	0.834 B	21.35 B	13.00 B	24.50 B	–	1.84 AB	36.23B	6.61 B	7.82 B
	T3	7.19 C	1.28 C	5.49 C	0.815 B	5.14 C	3.260 C	3.66 C	–	1.69 B	9.35 C	2.68 C	2.62 C
$LSD_{0.05}$		0.327	0.454	0.692	0.080	0.561	0.892	0.421	–	0.566	1.015	0.286	0.282
Lavender	T1	8.63 A	9.20 A	76.56 A	0.970 A	14.79 AB	16.43 A	42.83A	–	2.82A	64.1 A	20.84 A	22.65 A
	T2	7.84 B	6.03 B	26.39 B	0.796 B	21.20 A	14.15 B	24.35B	–	2.18B	36.0 B	6.28 B	7.41 B
	T3	7.16 C	1.41 C	5.25 C	0.830 B	5.65 B	3.62 C	3.19C	–	1.99C	10.17 C	2.44 C	2.29 C
$LSD_{0.05}$		0.096	0.461	1.67	0.065	11.58	0.873	10.45	–	0.12	11.85	1.81	1.79

Explanations as in Table 4.
Source: own study.

Table 7. Effect of irrigation water salinity on some heavy metals and non-metal contents in soil (mean, n = 10)

Plant name	Irrigation water type	B	Ba	Cd	Co	Cr	Cu	Fe	Mn	Ni	Mo	Pb	Sr	Zn
		ppm												
Sweet basil	T1	1.1268 A	31.35 A	0.290 A	3.65 A	50.15 A	160.10 A	5441.9 A	196.44 A	16.05 A	5.56 A	22.16 A	27.74 A	112.22 A
	T2	0.806 B	24.70 B	0.161 B	2.29 B	44.46 B	50.75 B	4193.5 B	186.74 B	15.06 A	5.59 A	15.16 C	23.70 B	106.49 B
	T3	0.476 C	22.60 B	0.173 B	1.34 C	39.80 C	26.20 C	4022.1 C	188.15 B	15.34 A	4.21 B	17.51 B	17.00 C	102.0 C
$LSD_{0.05}$		4.396	2.877	0.077	0.284	1.669	0.840	130.11	2.286	1.271	0.606	1.083	0.855	3.106
Lavender	T1	0.501 A	109.60 A	0.269 A	1.698 A	41.50 A	996.75 A	4159.6 A	197.35 A	14.75 A	5.46 A	22.16 A	27.50 A	105.0 A
	T2	0.326 B	94.50 A	0.176 B	1.475 B	35.65 B	167.50 B	4014 B	124.52 C	14.75 A	4.06 B	15.16 C	23.90 B	65.22 B
	T3	0.272 C	28.80 B	0.020 C	1.245 C	34.60 B	159.35 C	3583 C	187.55 B	13.55 B	3.53B	16.94 B	14.90 C	49.88 C
$LSD_{0.05}$		3.114	18.53	0.016	0.081	2.209	2.010	71.84	2.58	1.165	0.921	1.258	1.301	2.651

Explanations as in Table 4.
Source: own study.

EFFECT OF IRRIGATION WATER SALINITY ON EXTRACT OF SOIL PASTE

It is clear form Table 6 that increasing of the irrigation water salinity resulted in an increasing in soil reaction, soil electrical conductivity (*EC*), soil sodium adsorption ratio (*SAR*), exchangeable sodium percent (*ESP*) and soil contents of Na^+, K^+, Ca^{2+}, Mg^{2+}, Cl^- and SO_4^{2-}. Both of sodium adsorption ratio and exchangeable sodium percent were significantly affected by different treatments. *SAR* and *ESP* increased with increasing irrigation water salinity value. The highest values in this respect were noticed with salt water treatment (22.45 and 24.16) and (20.84 and 22.65) for sweet basil and lavender, respectively. The pH and *EC* of soil paste were decreased significantly in rhizosphere of plants irrigated with desalinated water. Also, *SAR* and *ESP* were decreased by 70.7 and 67.6 and 69.9 and 67.3 in rhizosphere soil of sweet basil and lavender, respectively.

Sodium and potassium ion content in rhizosphere soil of both tested plants were significantly increased with increasing salinity of irrigation water. In contrast, the highest calcium content was recorded in rhizosphere of plants irrigated with desalinated water followed by those irrigated with salt water and tap water.

EFFECT OF IRRIGATION WATER SALINITY ON SOME SOIL HEAVY METALS CONTENT

Some of heavy metals are considered very toxic even at low concentrations and may cause a great threat to the food chain and are completely dangerous at high levels [MUDGAL *et al*. 2010]. Data presented in Table 7 indicated that there was a significant decrease in heavy metal content in rhizosphere of both tested plants irrigated with desalinated water and tap water when compared with plants irrigated with salt water.

A slight excess of boron and strontium in the irrigation water or in the soil solution can cause toxicity to a variety of crops. Boron is taken up by the crop and is accumulated. Other constituents of some irrigation water, such as cobalt, molybdenum, lead and chromium may have deleterious effects on plants or animals even at very low concentration [GRATTAN *et al*. 2015]. Sodic soils have an *ESP* > 15, the EC_e is <4 dS m^{-1}, and the lower limit of the saturation extract SAR is 13. Consequently, Na^+ is the major problem in these soils [GHASSEMI *et al*. 1995].

CONCLUSIONS

It could be concluded that, the application of myco-synthesized AgNPs in thin film composite (TFC) membrane production reduced the cost of production and enhanced its performance (high flux and high rejection). The myco-synthesized AgNPs also showed strong inhibitory effect against common food-borne pathogens thereby the incorporation of such nanoparticles in composite membrane could reduce the biofouling of such membrane resulted from the formation of bacterial biofilm on membrane surface. The myco-synthesized AgNPs produced membrane thin film nanocomposite (TFNC) can produce water for irrigation with appreciated levels of nutrient ions and a minimum levels in the sodium absorption ratio and consequently alleviated the deleterious effects of salinity on plant and increased its productivity. In addition, the application of myco-synthesized AgNPs produced membrane in water desalination reduced the heavy metals content in water and hence their uptake by plants irrigated with desalinated water.

REFERENCES

AHLUWALIA V., KUMAR J., SISODIA R., SHAKIL N.A., WALIA S. 2014. Green synthesis of silver nanoparticles by *Trichoderma harzianum* and their bio-efficacy evaluation against *Staphylococcus aureus* and *Klebsiella pneumonia*. Industrial Crops and Products. Vol. 55 p. 202–206. DOI 10.1016/j.indcrop.2014.01.026.

AL-KARAGHOULI A., RENNE D., KAZMERSKI L.L. 2009. Solar and wind opportunities for waterdesalination in the Arab regions. Renewable and Sustainable Energy Reviews. Vol. 13. Iss. 9 p. 2397–2407. DOI 10.1016/j.rser.2008.05.007.

ASHRAF M., SHAHZAD S.M., AKHTAR N., IMTIAZ M., ALI A. 2016. Salinization/sodification of soil and physiological dynamics of sunflower irrigated with saline–sodic water amending by potassium and farm yard manure. Journal of Water Reuse and Desalination. Vol. 7. Iss. 4 p. 476–487. DOI 10.2166/wrd.2016.053.

BELTRÁN J.M., KOO-OSHIMA S. 2006. Water desalination for agricultural applications. Land and Water Discussion Paper. No. 5. Proceedings of the FAO Expert Consultation on Water Desalination for Agricultural Applications. 26–27 April 2004, Rome. Rome. FAO pp. 48.

EL-AASSAR A.M., ELFADL M.M.A., ALI M.E., KOTP Y.H., SHAWKY H.A. 2017. Effect of manufacture conditions on reverse osmosis desalination performance of polyamide thin film composite membrane and their spiral wound element.

Desalination and Water Treatment. Vol. 22. Iss. 26 p. 65–71. DOI 10.5004/dwt.2017.20293.

FOUDAA A., SAAD E.L., ELGAMALA M.S., MOHMEDB A.A., SALEMA S.S. 2017. Optimal factors for biosynthesis of silver nanoparticles by *Aspergillus* sp. Al Azhar Bulletin of Science. Vol. 9 p. 161–172.

GAUR A., ADHOLEYA A. 2004. Prospects of arbuscular mycorrhizal fungi in phytoremediation of heavy metal contaminated soils. Current Science. Vol. 86. Iss. 4 p. 528–534.

GHASSEMI F., JAKEMAN A.J., NIX H.A.1996. Salinisation of land and water resources: Human causes, extent, management and case studies. Australian Geographical Studies. Vol. 34. Iss. 1 p. 159–161.

GRATTAN S.R., DÍAZ F.J., PEDRERO F., VIVALDI G.A. 2015. Assessing the suitability of saline wastewaters for irrigation of *Citrus* spp.: Emphasis on boron and specific-ion interactions. Agricultural Water Management. Vol. 157 p. 48–58. DOI 10.1016/j.agwat.2015.01.002.

GUILGER-CASAGRANDE M., GERMANO-COSTA T., PASQUOTO-STIGLIANI T., FRACETO L.F., DE LIMA R. 2019. Biosynthesis of silver nanoparticles employing *Trichoderma harzianum* with enzymatic stimulation for the control of *Sclerotinia sclerotiorum*. Scientific Reports. Vol. 9. Iss. 1 p. 1–9. DOI 10.1038/s41598-019-50871-0.

HAMEDI S., GHASEMINEZHAD S., SHOJAOSADATI S., SHOKROLLAHZADEH S. 2012. Comparative study on silver nanoparticles properties produced by green methods. Iranian Journal of Biotechnology. Vol. 10. Iss. 3 p. 191–197.

HARLEYS. M. 1993. Use of a simple, colorimetric assay to demonstrate conditions for induction of nitrate reductase in plants. American Biology Teacher. Vol. 55. Iss. 3 p. 162–164. DOI 10.2307/4449615.

KLEIN D.A., LOH T.C., GOULDING R.L. 1971. A rapid procedure to evaluate the dehydrogenase activity of soils low in organic matter. Soil Biology and Biochemistry. Vol. 3. Iss. 4 p. 385–387. DOI 10.1016/0038-0717(71)90049-6.

KOTP Y.H. 2017. Controlled synthesis and sorption properties of magnesium silicate nanoflower prepared by a surfactant-mediated method. Separation Science and Technology. Vol. 52. Iss. 4 p. 657–670. DOI 10.1080/01496395.2016.1264425.

KOTP Y.H., SHEBL Y.A., EL-DEAB M.S., EL-ANADOULI B.E., SHAWKY H.A. 2017. Performance enhancement of PA-TFC RO membrane by using magnesium silicate nanoparticles. Journal of Inorganic and Organometallic Polymers and Materials. Vol. 27. Iss. 1 p. 201–214. DOI 10.1007/s10904-017-0667-9.

LEÓN-ROMERO M.A., SOTO-RÍOS P.C., FUJIBAYASHI M., NISHIMURA O. 2017. Impact of NaCl solution pretreatment on plant growth and the uptake of multi-heavy metal by the model plant *Arabidopsis thaliana*. Water, Air, and Soil Pollution. Vol. 228. Iss. 2 p. 64. DOI 10.1007/s11270-017-3241-8.

MUDGAL V., MADAAN N., MUDGALA. 2010. Heavy metals in plants: phytoremediation: plants used to remediate heavy metal pollution. Agriculture and Biology Journal of North America. Recent Patents on Nanotechnology. Vol. 1. Iss. 1 p. 40–46.

NICOLÁS E. 2019. Ripening indices, olive yield and oil quality in response to irrigation with saline reclaimed water and deficit strategies. Frontiers in Plant Science. Vol. 10, 1243. DOI 10.3389/fpls.2019.01243.

OTTONI C.A., SIMÕES M.F., FERNANDES S., DOS SANTOS J.G., DA SILVA E.S., DE SOUZA R.F.B., MAIORANO A.E. 2017. Screening of filamentous fungi for antimicrobial silver nanoparticles synthesis. AMB Express. Vol. 7. Iss. 1, 31. DOI 10.1186/s13568-017-0332-2.

PITT J., HOCKING A. 2009. Fungi and food spoilage. Dordrecht Heidelberg London New York. Springer. ISBN 978-0-387-92206-5 pp. 520.

REHAN Z.A., GZARA L., KHAN S.B., ALAMRY K.A., EL-SHAHAWI M.S., ALBEIRUTTY M.H., FIGOLI A., DRIOLI E., ASIRI A.M. 2016. Synthesis and characterization of silver nanoparticles-filled polyethersulfone membranes for antibacterial and anti-biofouling application. Recent Patents on Nanotechnology. Vol. 10. Iss. 3 p. 231–251. DOI 10.2174/1872210510666160429145228.

SANGAPPA M., THIAGARAJAN P. 2012. Mycobiosynthesis and characterization of silver nanoparticles from *Aspergillus niger*: A soil fungal isolate. International Journal of Life Sciences Biotechnology and Pharma Research. Vol. 1. Iss. 2 p. 282–289.

SOLIMAN E.R., KOTP Y.H., SOUAYA E.R., GUINDY K.A., IBRAHIM R.G. 2019. Development the sorption behavior of nanocomposite Mg/Al LDH by chelating with different monomers. Composites. Part B: Engineering. Vol. 175, 107131. DOI 10.1016/j.compositesb.2019.107131.

SRIDHAR S., AMINABHAVI T.M., MAYOR S.J., RAMAKRISHNA M. 2007. Permeation of carbon dioxide and methane gases through novel silver-incorporated thin film composite pebax membranes. Industrial and Engineering Chemistry Research. Vol. 46. Iss. 24 p. 8144–8151. DOI 10.1021/ie070114k.

USDA 2014. Kellogg Soil Survey Laboratory Methods Manual. Soil Survey Investigations Report. No. 42 Ver. 5.0. United States Department of Agriculture pp. 1001.

VRIJENHOEK E.M., HONG S., ELIMELECH M. 2001. Influence of membrane surface properties on initial rate of colloidal fouling of reverse osmosis and nanofiltration membranes. Journal of Membrane Science. Vol. 188. Iss. 1 p. 115–128. DOI 10.1016/S0376-7388(01)00376-3.

WEI W., BILSBORROW P.E., HOOLEY P., FINCHAM D.A., LOMBI E., FORSTER B.P. 2003. Salinity induced differences in growth, ion distribution and partitioning in barley between the cultivar Maythorpe and its derived mutant Golden Promise. Plant and Soil. Vol. 250. Iss. 2 p. 183–191. DOI 10.1023/A:1022832107999.

WHO 2006. Guidelines for assessing quality of herbal medicines with reference to contaminants and residues. Geneva, Switzerland. World Health Organization. ISBN 9789241594448 pp. 105.

YASEEN R., YOSSIF T. 2019. Functional microbial diversity in relation to soil characteristics and land uses of Wadi Um Ashtan Basin, North-western Coast, Egypt. Egyptian Journal of Soil Science. Vol. 59. Iss. 3 p. 287–297. DOI 10.21608/EJSS.2019.14096.1282.

YIN J., YANG Y., HU Z., DENG B.2013. Attachment of silver nanoparticles (AgNPs) onto thin-film composite (TFC) membranes through covalent bonding to reduce membrane biofouling. Journal of Membrane Science. Vol. 441 p. 73–82. DOI 10.1016/j.memsci.2013.03.060.